U.S. DEPARTMENT OF ENERGY | Energy Efficiency & Renewable Energy

BUILDING TECHNOLOGIES PROGRAM

Laboratory Test Report for Fujitsu 12RLS and Mitsubishi FE12NA Mini-Split Heat Pumps

Jon Winkler, Ph.D.

September 2011

Building America
U.S. Department of Energy

Available electronically at http://www.osti.gov/bridge

Available for a processing fee to U.S. Department of Energy
and its contractors, in paper, from:
U.S. Department of Energy
Office of Scientific and Technical Information
P.O. Box 62
Oak Ridge, TN 37831-0062
phone: 865.576.8401
fax: 865.576.5728
email: mailto:reports@adonis.osti.gov

Available for sale to the public, in paper, from:
U.S. Department of Commerce
National Technical Information Service
5285 Port Royal Road
Springfield, VA 22161
phone: 800.553.6847
fax: 703.605.6900
email: orders@ntis.fedworld.gov
online ordering: http://www.ntis.gov/ordering.htm

Printed on paper containing at least 50% wastepaper, including 20% postconsumer waste

Laboratory Test Report for Fujitsu 12RLS and Mitsubishi FE12NA Mini-Split Heat Pumps

Prepared for:

Building America

Building Technologies Program

Office of Energy Efficiency and Renewable Energy

U.S. Department of Energy

Prepared by:

Jon Winkler

National Renewable Energy Laboratory

1617 Cole Boulevard

Golden, CO 80401-3393

September 2011

[This page left blank]

Contents

List of Figures

List of Tables

Definitions

AHRI	Air-Conditioning, Heating, and Refrigeration Institute
ASHRAE	American Society of Heating, Refrigerating, and Air-Conditioning Engineers
Btu	British thermal unit
cfm	cubic feet per minute
COP	coefficient of performance
DB	dry-bulb
EER	energy efficiency ratio
HSPF	heating seasonal performance factor
HVAC	heating, ventilating, and air conditioning
MSHP	mini-split heat pump
NEEA	Northwest Energy Efficiency Alliance
SEER	seasonal energy efficiency ratio
W	watt
WB	wet-bulb

U.S. DEPARTMENT OF ENERGY | Energy Efficiency & Renewable Energy

Executive Summary and Acknowledgments

Mini-split heat pumps are being proposed as a new retrofit option to replace resistance heating in the Pacific Northwest. NREL has previously developed a field test protocol for mini-split systems to ensure consistent results from field tests (Christensen et al. 2011). This report focuses on the development of detailed system performance maps for mini-split heat pumps to expand on data reported by manufacturers so that the cost and performance characteristics of mini-split systems can be accurately compared with conventional systems. This report presents laboratory test results for two mini-split heat pumps. Steady-state heating and cooling performance for the Fujitsu 12RLS and Mitsubishi FE12NA was tested under a wide range of outdoor and indoor temperatures at various compressor and fan speeds. Cycling performance for each unit was also tested under both modes of operation. The experimental test data aligned with manufacturer reported values and both systems outperformed two-stage, high SEER forced air systems under low and intermediate loads. However, high SEER forced air systems tend to have slightly higher (10%–25%) COPs when operating at peak load. Adequate datasets were attained to promote performance modeling of these two systems in the future.

This work was carried out in partnership with Ecotope, Inc. and researchers at the Purdue University Herrick Laboratories. The author would like to thank Ben Larson of Ecotope, Inc. and Jim Braun and Howard Cheung of Herrick Laboratories for their support and for attaining high quality data. The data presented in this report are also presented by Larson et al. (2011).

1 Project Overview

Mini-split heat pumps (MSHPs) have several potential benefits over conventional heating, ventilating, and air-conditioning (HVAC) systems for use in both newly constructed energy efficient homes and in older home retrofits. By controlling the temperature and humidity in each zone, MSHPs offer energy savings by only conditioning occupied rooms instead of an entire house. High end mini-split heat pump technologies utilize variable speed compressors and fans allowing for a reduction in cycling losses, improved part load control, and enhanced humidity control. The ductless nature of these systems also reduces air-side losses. A ductless system could be particularly useful in retrofit applications where ductwork might not be available or easily installed.

Several issues must be resolved before MSHPs can achieve broad market penetration in the U.S. MSHPs are likely more expensive than high seasonal energy efficiency ratio (SEER) forced air systems; particularly when installed in an average size U.S. home which will typically require multiple indoor units. However, a detailed cost analysis comparing high SEER forced air systems with ducts in conditioned space to MSHP options needs to be conducted. Homeowners may not prefer wall mounted MSHPs for aesthetic reasons. Aesthetic issues could potentially be minimized by using ceiling mounted or ceiling cassette indoor units. It may also be more difficult to install indoor units in every room than installing supply air registers, particularly in new construction. Due to the expense and difficulty of installing an indoor unit in every room, some rooms may not be directly conditioned, leading to reduced comfort compared to forced air systems.

Several mini-split heat pumps currently on the market are rated at SEER 25 or above. These impressive ratings, compared to high SEER forced air systems (SEER 18 and above), potentially make MSHPs a promising space conditioning solution for reducing the amount of energy used in residential buildings. In order to validate the potential benefit of these systems, it is first essential to increase the knowledge and understanding of how they will perform in a variety of operating conditions and climate types. This can only be achieved through laboratory experiments and field monitoring of installed units. Laboratory experimentation provides controlled and accurate performance data against which installed performance from real homes can be compared and component models for use in whole-house simulation tools can be generated. MSHP manufacturers publish performance data for a single speed only and do not publish sufficient data for performance map and component model development.

This project originated with the Northwest Energy Efficiency Alliance (NEEA) funding Ecotope, Inc. to evaluate the Northwest Ductless Heat Pump Pilot Project. The original scope included field monitoring of 95 MSHP installations throughout the Pacific Northwest and laboratory performance testing of two MSHPs conducted by Herrick Laboratories at Purdue University. The National Renewable Energy Laboratory (NREL) has funded laboratory testing of three additional MSHPs which is currently underway. This report publishes experimental performance testing of two MSHPs, the Fujitsu 12RLS and Mitsubishi FE12NA, originally sponsored by NEEA. Laboratory test data for the three additional units are scheduled to be published in Fall 2012. Table 1 compares manufacturer published data for the two units included in this report.

Table 1 includes the individual model numbers for the indoor and outdoor units for each system. Both systems were tested using wall mounted indoor units.

Table 1. Comparison of Manufacturer Reported Data

		Fujitsu 12RLS	Mitsubishi FE12NA
Outdoor Unit	–	ASU12RLS	MUZ-FE12NA
Indoor Unit	–	AOU12RLS	MSZ-FE12NA
Seasonal energy-efficiency ratio (SEER)	Btu/h-W	25	23
Heating seasonal performance factor (HSPF)	Btu/h-W	12	10.6
Rated cooling capacity	Btu/h	12,000	12,000
Cooling capacity range	Btu/h	3,800–14,500	2,800–12,000
Cooling energy efficiency ratio (EER)	Btu/h-W	14.46	12.9
Rated heating capacity	Btu/h	16,000	13,600
Heating capacity range	Btu/h	3,100–24,000	3,000–21,000
Heating coefficient of performance (COP)	–	3.9	4.2

Sources: Fujitsu 2009, Mitsubishi 2009a, Mitsubishi 2009b

2 Test Description

Both MSHPs were tested by Herrick Laboratories at the Mechanical Engineering Department at Purdue University. The units were tested under a variety of operating conditions and measurements were taken to characterize and map the performance of both heat pumps. The MSHP performance maps will be used to explain trends that were witnessed in the field during the data monitoring process and will be used to develop component models for whole house simulation tools.

2.1 Experimental Test Facility

Herrick Laboratories has two American Society of Heating, Refrigerating, and Air-Conditioning Engineers (ASHRAE) standard psychrometric chambers designed to test HVAC equipment. These chambers consist of two highly insulated rooms capable of controlling temperature and humidity to simulate indoor and outdoor temperature and humidity conditions. The indoor room is equipped with an ASHRAE standard air measurement box to measure the indoor unit airflow rate (ASHRAE 1987). Figure 1 displays the outdoor and indoor units of the Fujitsu system instrumented in the respective psychrometric chambers. An insulated discharge plenum was constructed surrounding the outlet of the indoor coil to measure the exiting dry-bulb (DB) temperatures.

NREL/PIX 19345 (left), 19343 (right)
Credit: Howard Cheung/Herrick Labs

Figure 1. Instrumented outdoor unit (left) and instrumented indoor unit (right) covered by insulated discharge plenum

2.2 Measurements

Measurements included the following:

- Fan power and speed for both the indoor and outdoor heat exchangers
- Total heat pump power and auxiliary power
- Refrigerant mass flow rate
- Refrigerant pressures and temperatures measured at the compressor suction line, compressor discharge line, liquid line, and inlet to the evaporator
- Indoor coil return (inlet) air temperature, pressure, and humidity
- Indoor coil supply (outlet) air temperature, pressure, humidity, and volumetric flow rate

- Outdoor coil inlet and outlet temperatures
- Condensate flow rate
- Mode of operation
- Thermostat set point.

The air volumetric flow rate was determined by measuring the pressure drop across a calibrated nozzle. The air was directed across the nozzle using a discharge plenum (shown in Figure 1). The indoor fan power and air-side pressure drop were measured prior to connecting the discharge plenum to determine the free stream fan performance. The lab added a booster fan to the discharge plenum to cancel out the external static pressure associated with the plenum and the booster fan flow rate was adjusted to match the indoor unit fan power to the free stream fan power.

2.3 Heating Mode Tests

Heating mode tests included steady-state, cyclic, and defrost tests. The purpose of the steady-state tests is to acquire a sufficient amount of data to develop accurate performance maps. The test matrix was designed to optimize test time while testing each unit under a variety of operating conditions. Under certain operating conditions in heating mode, frost will accumulate on the outdoor heat exchanger and the unit must enter a defrost cycle to melt the accumulated frost. The unit's efficiency during defrost operation is taken into account in HSPF calculations. MSHPs don't often cycle between on and off due to the variable speed control, however, the HSPF calculation is also dependent on cycling performance degradation.

For each operating condition, various fan and compressor speeds were tested. Fan speed was set using the high, medium, or low setting on the unit's remote control. The compressor speed was varied indirectly by varying the load provided by the psychrometric chamber and the thermostat setting on the unit's remote control. A majority of the tests were conducted at an indoor temperature of 70°F. Several test points at different indoor temperatures were added to capture the dependence of return air temperature on the heat pump performance. Herrick Laboratories tested the Fujitsu unit first. Slight improvements were made to the steady-state heating mode test matrix for the Mitsubishi unit as more was understood about MSHP behavior. The cyclic and defrost tests are required to calculate the HSPF as outlined by Air-Conditioning, Heating, and Refrigeration Institute (AHRI) Standard 210/240 (AHRI 2008).

Test codes were developed to distinguish between different test points. An example test code is shown in Figure 2. The first letter in the test code distinguishes between heating and cooling operation and the second entry describes the type of test. This is followed by the intended outdoor temperature, fan speed, and compressor speed, respectively. The default return dry-bulb temperature for heating mode is 70°F and the default return wet-bulb (WB) for cooling mode is 67°F. The final entry in the test code is included if the test was conducted at an intended indoor condition other than the default value. This field is left blank if the test was conducted using the standard temperature.

H	-	SS	-	47	-	H	-	MX	-	_ _
Operation		Test Mode		Outdoor Temperature		Fan Speed		Compressor Speed		Return Dry Bulb (Heating) *or* Return Wet Bulb (Cooling)
• H = Heating • C = Cooling		• SS = Steady State • DF = Defrost • CY = Cycling				• H = High • M = Medium • L = Low		• MX = Maximum • INT = Intermediate • MN = Minimum		

Figure 2. Experimental test code description

Each test code denotes the intended indoor and outdoor temperatures. The laboratory did not always hit the intended temperature, but the actual chamber temperature (and not the intended temperature) will be used for data analysis and performance model development. Thus, it was not crucial that the actual chamber conditions matched the intended conditions perfectly.

2.4 Cooling Mode Tests

Cooling mode tests included steady-state and cyclic tests. Similar to the heating mode tests, a variety of operating conditions were tested to best characterize the performance of the system under different indoor and outdoor temperatures, fan speeds, and cooling loads. The indoor wet-bulb temperature becomes an important variable when switching to cooling mode. A majority of the test points were conducted at 80°F dry-bulb and 67°F wet-bulb indoor condition since this is the indoor operating condition used by the SEER rating procedure for steady state tests. Additional test points were added to the FE12NA test matrix after it was determined more points were needed to accurately model the cooling performance.

3 Airflow Measurements

Table 2 compares the indoor airflow rates achieved in the laboratory to the manufacturer-reported data. The experimental values listed are the average values from the set of experiments for the given fan speed. There are discrepancies between the manufacturer-reported and the experimentally determined values for both units at several modes of operation. However, most measured airflow rates align with the manufacturer reported values. The heating and cooling steady-state test data for both units are included in Appendix A. The indoor fan airflow rate and power varied slightly for a given speed setting and test.

Table 2. Experimental Indoor Fan Performance Compared to Manufacturer Reported Values

	Manufacturer-Reported Values*			Experimental Values			
	Fan Speed	Airflow Rate (cfm)		Airflow Rate (cfm)		Fan Power (W)	
		Heating	Cooling	Heating	Cooling	Heating	Cooling
12RLS	High	453		426	475	28	38
	Medium	374		348	390	20	25
	Low	274		250	286	12	14
FE12NA	High	399	350	338	338	24	23
	Medium	240	202	233	204	12	9
	Low	166	144	149	144	6	5

***Sources: Fujitsu 2009 and Mitsubishi 2009a**

The indoor fans for both units are very efficient. The efficiency ranged from approximately 0.04 W/cfm to 0.08 W/cfm. The high fan efficiency can be attributed to the ductless nature of these systems since the return and supply air streams are in free space and are not burdened by the external static pressure associated with ductwork.

4 Heating Test Results

The air-side and refrigerant-side capacities of the indoor coil were determined for each test and ASHRAE Standard 116 mandates that the two capacities be within 6% of each other (ASHRAE 2010). However, the refrigerant-side capacity can only be determined if the refrigerant exiting the condenser is subcooled liquid and the refrigerant exiting the evaporator is superheated vapor. These conditions were not present for all steady-state tests, however, the air-side and refrigerant-side capacities were within 6% of each other for all cases in which the refrigerant-side capacity could be determined. Since the air-side and refrigerant-side capacities were always within 6% of each other, the air-side capacity measurement was deemed reliable when the refrigerant-side capacity could not be determined.

4.1 Steady State – Fujitsu 12RLS

Steady-state heating results for the Fujitsu 12RLS with a 70°F return dry-bulb temperature are displayed in Figure 3.

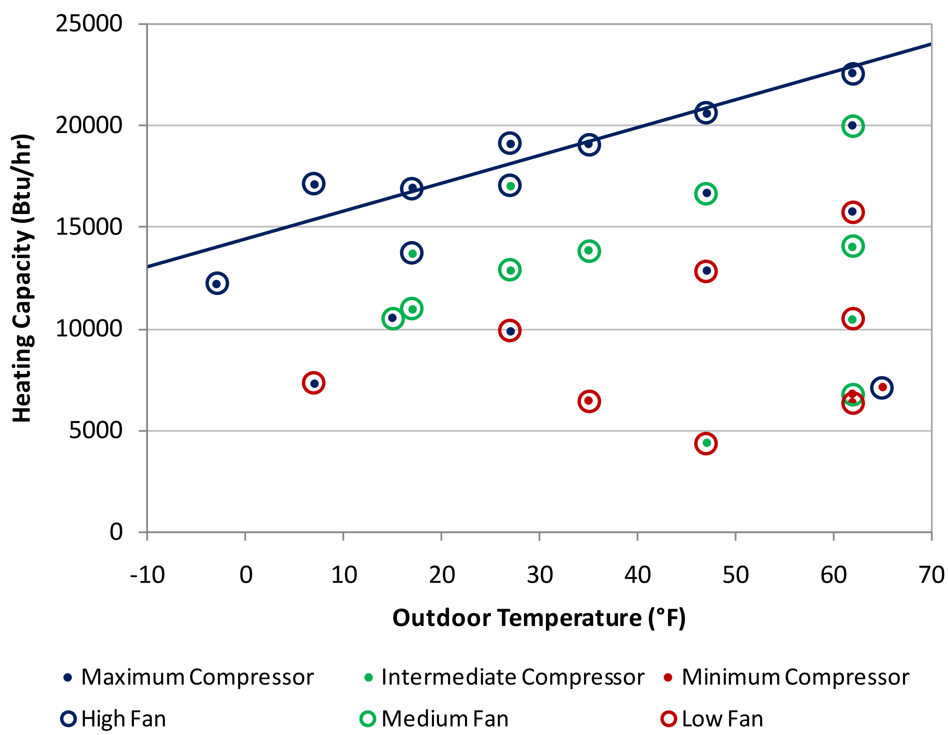

Figure 3. Fujitsu 12RLS steady-state heating capacities (70°F return temperature)

The data cover a large range of outside temperatures and operating modes. The open circles denote the fan speed and the closed dots denote the compressor speed/load for the given test point. The fan speed was set using the indoor unit's remote control. Maximum and minimum compressor speeds were achieved using manufacturer recommendations. Since both units include a variable speed compressor, many intermediate speeds exist between the minimum and maximum speed. Thus, the intermediate compressor speed/load results included in this report may not align with the intermediate load data provided by manufacturers.

Various combinations of fan and compressor speeds were tested. The unit was most commonly tested at a high fan speed under full load and a trend line was added to these points to highlight the effect of outdoor temperature on heat pump capacity. As expected, the heat pump capacity decreases with decreasing outdoor temperature. Stated previously in Table 1, the rated heating capacity for this unit was 16,000 Btu/h at 47°F and the trend line shows the rated capacity can be achieved to approximately 7°F. The scatter in the plot exemplifies the variable speed nature of the heat pump and the ability of the heat pump to meet various heating loads without cycling on and off. The manufacturer claims the heating capacity can vary from 3,100–24,000 Btu/h, however, despite loading the compressor to achieve minimum operation based on the manufacturer recommendations, this minimum capacity was not observed in the laboratory. Thus based on the behavior observed in the laboratory, the unit would need to cycle on and off to meet a load lower than approximately 5,000 Btu/h.

Figure 4 compares the manufacturer-reported heating capacity to the laboratory test data. The manufacturer-reported data correspond to a high fan speed under an intermediate load. This combination of fan speed and load was not commonly tested in the laboratory, but high fan speed under full load operation is plotted in Figure 4 for comparison. Thus, it is not surprising that the laboratory capacities shown in Figure 4 are higher than the manufacturer-reported data. The manufacturer-reported heating capacities align with the experimental results plotted in Figure 3. The capacity degradation with colder outdoor temperatures is similar between the reported and laboratory data, as indicated by the slopes of the linear trend lines.

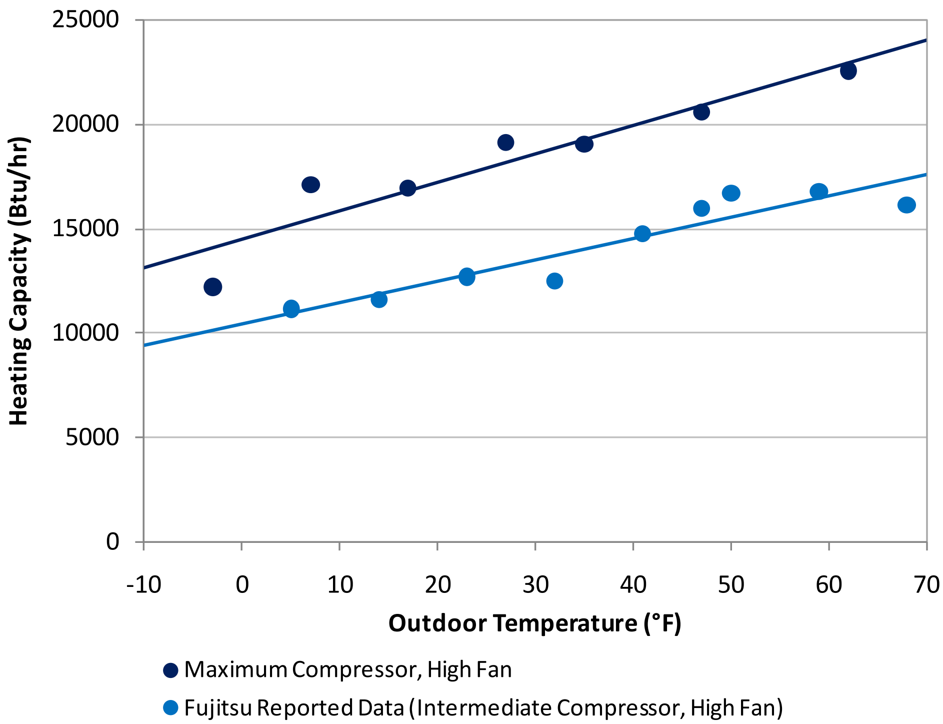

Figure 4. Fujitsu 12RLS maximum steady-state heating capacity compared to manufacturer-reported data (70°F return temperature)

Source: Fujitsu 2009

Figure 5 plots the heating coefficient of performance (COP) laboratory test results for a return temperature of 70°F. As expected, the COP decreases with lower outdoor temperature and higher COPs are achievable at low compressor loads (for a given outdoor temperature). For a given outdoor temperature and compressor speed, changing the fan speed has only a small effect on the COP. The higher fan speed leads to a small increase in capacity but the increase in fan power offsets the capacity increase for little effect on the COP.

Figure 6 compares the manufacturer-reported COP against the laboratory-tested COP for high fan speed, maximum compressor speed operation. Again, the manufacturer-reported data correspond to a high fan speed under an intermediate load, and this combination of fan speed and load was not commonly tested in the laboratory. However, high fan speed under full load operation is plotted in Figure 6 for comparison. It is expected that the manufacturer-reported COP is slightly higher in this case since the data are for an intermediate compressor load. The manufacturer-reported COPs in Figure 6 align with the values plotted in Figure 5.

Steady-state heating results for all laboratory tests of the Fujitsu 12RLS are included in Table 5 located in Appendix A. Table 5 includes the indoor fan power, outdoor unit total power, indoor airflow rate, and supply air temperature in addition to the heating capacity and COP.

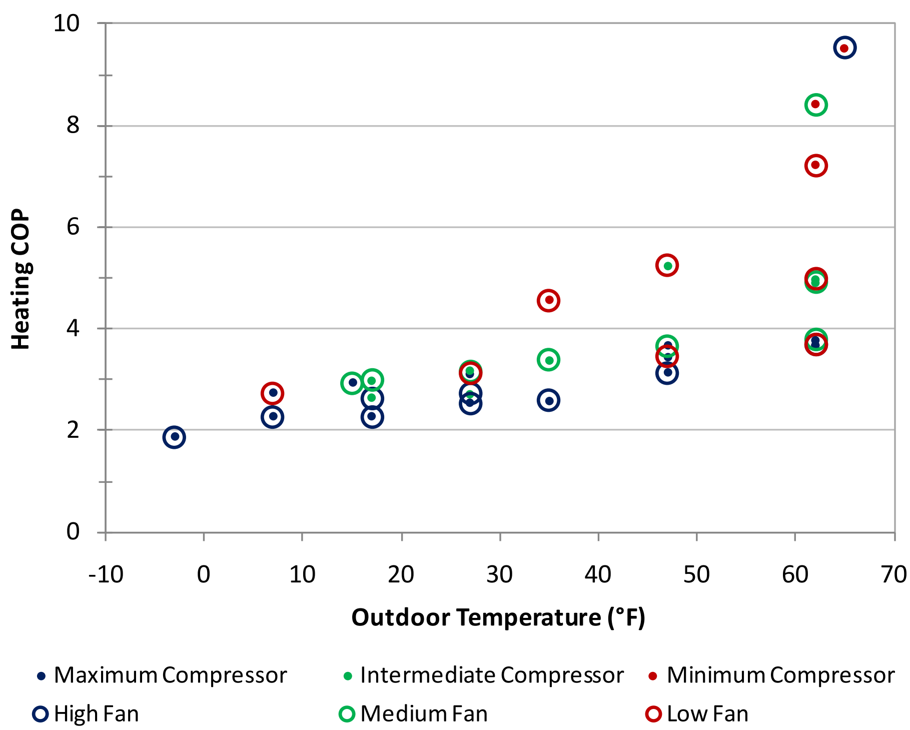

Figure 5. Fujitsu 12RLS steady-state heating COP (70°F return temperature)

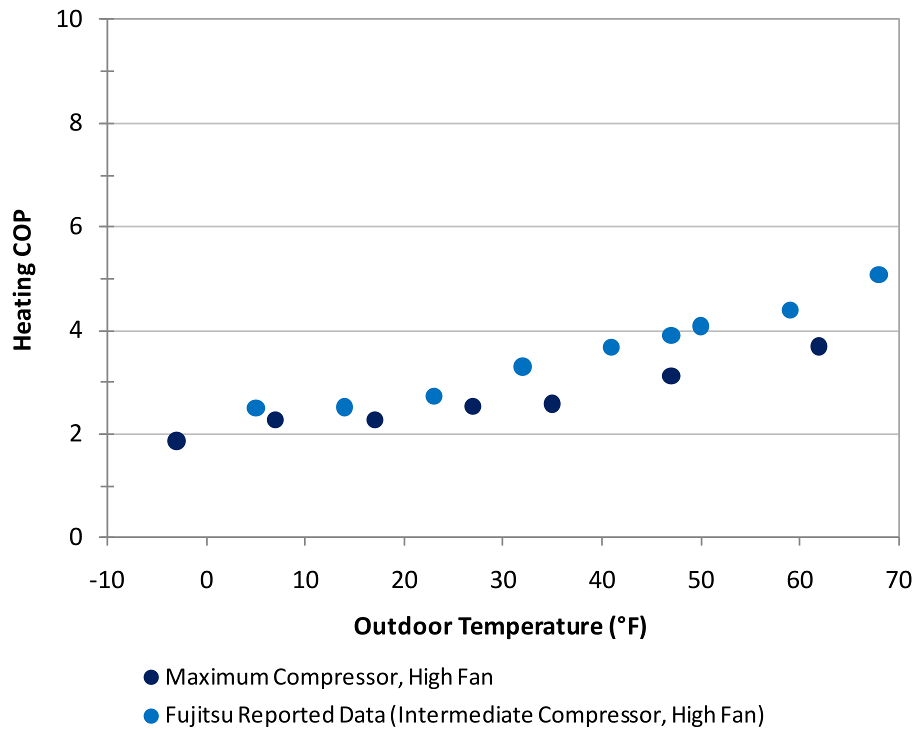

Figure 6. Fujitsu 12RLS heating COP compared to manufacturer-reported data (70°F return temperature)

Source: Fujitsu 2009

The data acquisition program failed to record the actual outdoor coil inlet air temperature during testing. This oversight was corrected prior to testing the Mitsubishi unit and did not affect the laboratory's ability to achieve acceptable energy balances. From the Mitsubishi unit test data, it was noticed that the actual chamber temperature was consistently lower than the intended temperature and this offset increased for colder intended temperatures. The actual outdoor coil inlet temperature equaled the intended temperature (an offset of 0°F) at a test condition of approximately 85°F and increased linearly to an offset of approximately 6°F at a test condition of -7°F. Since the actual outdoor coil inlet temperature was colder than intended, the reported experimental heating capacities would have been higher if actual inlet air temperature equaled the intended value. Thus, it is expected that the experimental heating capacities, at the temperatures plotted in Figure 3 and Figure 4, were higher than what is displayed.

4.2 Steady State – Mitsubishi FE12NA

Steady-state heating capacity results for the Mitsubishi FE12NA at a 70°F return temperature are displayed in Figure 7. Similar to Figure 3, the open circles denote fan speed and closed circles denote compressor speed for the given test point. A trend line has been added for the maximum compressor; high fan speed operating points. As shown in Table 1, the rated heating capacity for the FE12NA is 13,600 Btu/h, and based on the trend line, the rated capacity can be achieved to an approximate outdoor temperature of 18°F under full load conditions.

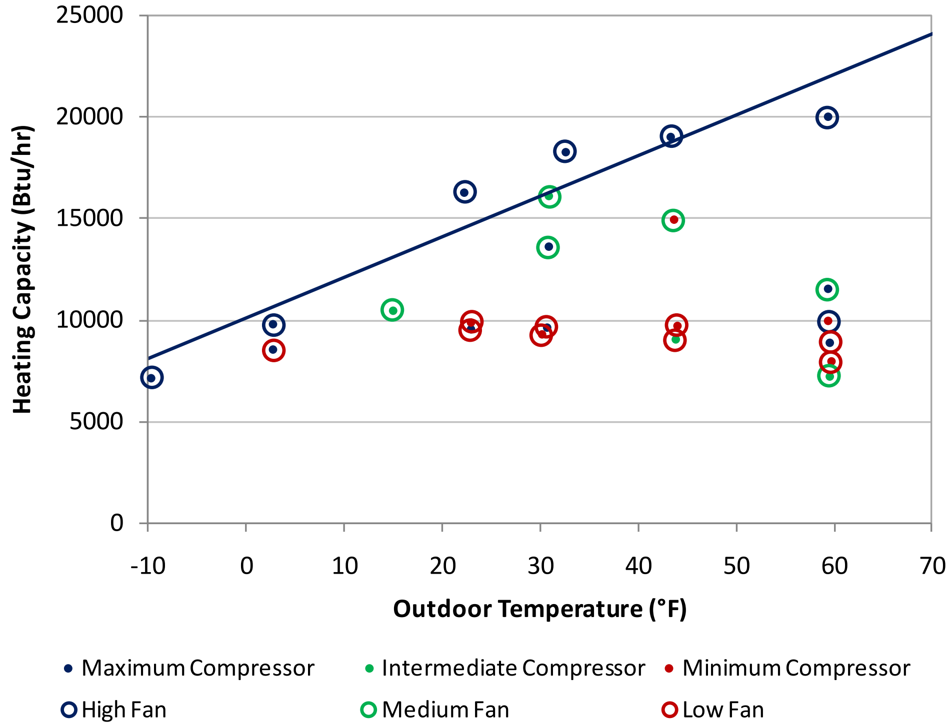

Figure 7. Mitsubishi FE12NA steady-state heating capacities (70°F return temperature)

Figure 8 compares the manufacturer-reported performance data to the laboratory test data. For the Mitsubishi-reported data, the unit operated at a high fan speed under an intermediate compressor load and the high fan speed, full compressor load laboratory data are plotted for comparison. Thus, it is not surprising that the Mitsubishi reported capacities were lower in this case.

Mitsubishi reported performance at various outdoor wet-bulb temperatures and did not list the coincident dry-bulb temperatures in the extended performance table. Therefore, assumptions had to be made to determine the corresponding dry-bulb temperatures to include in Figure 8 (and Figure 10) for comparison to the experimental data. The performance listed by Mitsubishi for the FE12NA was for heating operation without defrost (dry coil). The performance data for an outdoor wet-bulb temperature of 43°F equaled the performance at the rated operating condition (47 °F dry-bulb and 43°F wet-bulb) listed for the unit. Therefore, it was assumed the dew-point depression was constant for all listed wet-bulb temperatures allowing for the calculation of a coincident dry-bulb temperature. The capacity degradation with colder outside temperatures is similar between the reported and laboratory data, as indicated by the slopes of the linear trend lines. The capacity degradation with respect to colder outdoor temperatures appears greater compared to the Fujitsu unit.

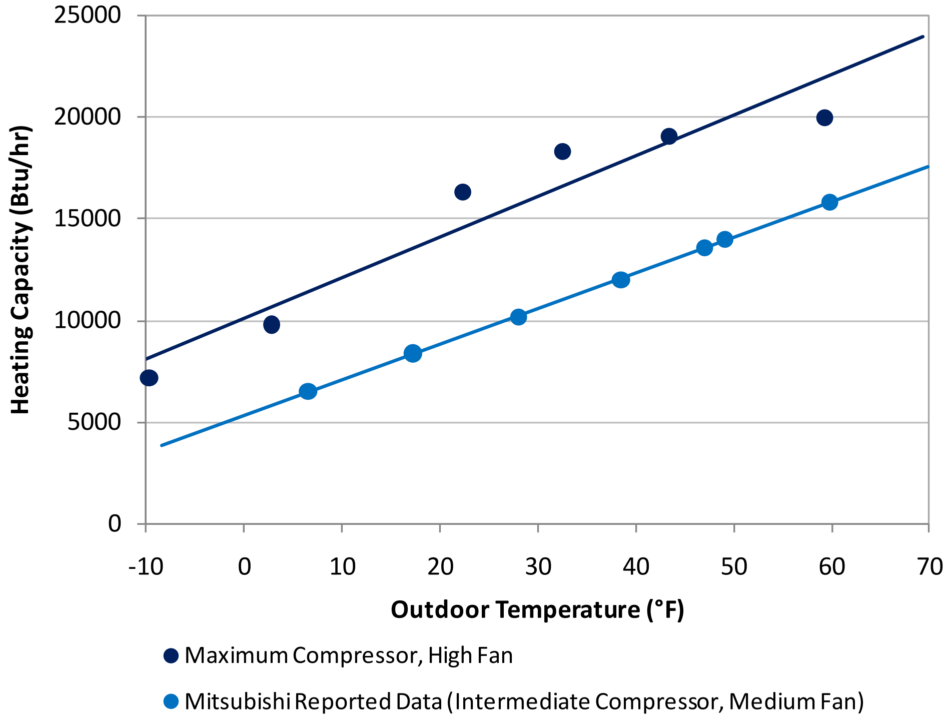

Figure 8. Mitsubishi FE12NA maximum steady-state heating capacity compared to manufacturer-reported data (70°F return temperature)

Source: Mitsubishi 2009b

Figure 9 plots the heating COP laboratory results for a return temperature of 70°F. The values and trends are similar to the results for the Fujitsu unit plotted in Figure 5. It would appear the Fujitsu unit has higher COPs at low compressor loads, but as previously mentioned, the Fujitsu unit also has a higher HSPF despite having a lower-rated COP. Figure 10 compares the manufacturer-reported COP against the laboratory-tested COP. It is expected that the manufacturer-reported COP is slightly higher in this case since the manufacturer-reported data are for an intermediate compressor load and the plotted laboratory data are for high fan speed, full compressor load operation.

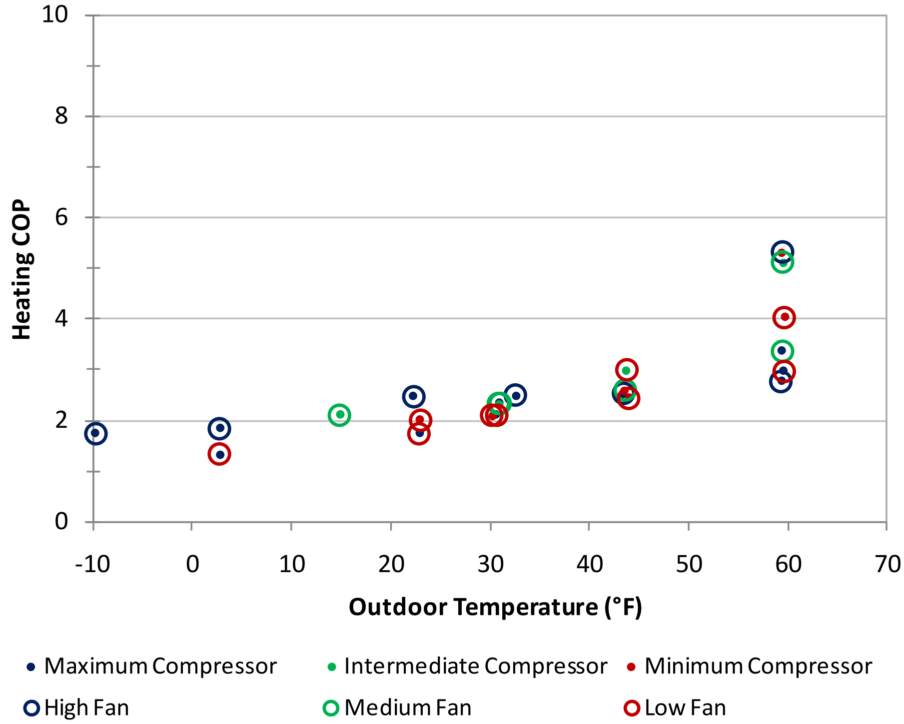

Figure 9. Mitsubishi FE12NA steady-state heating COP (70°F return temperature)

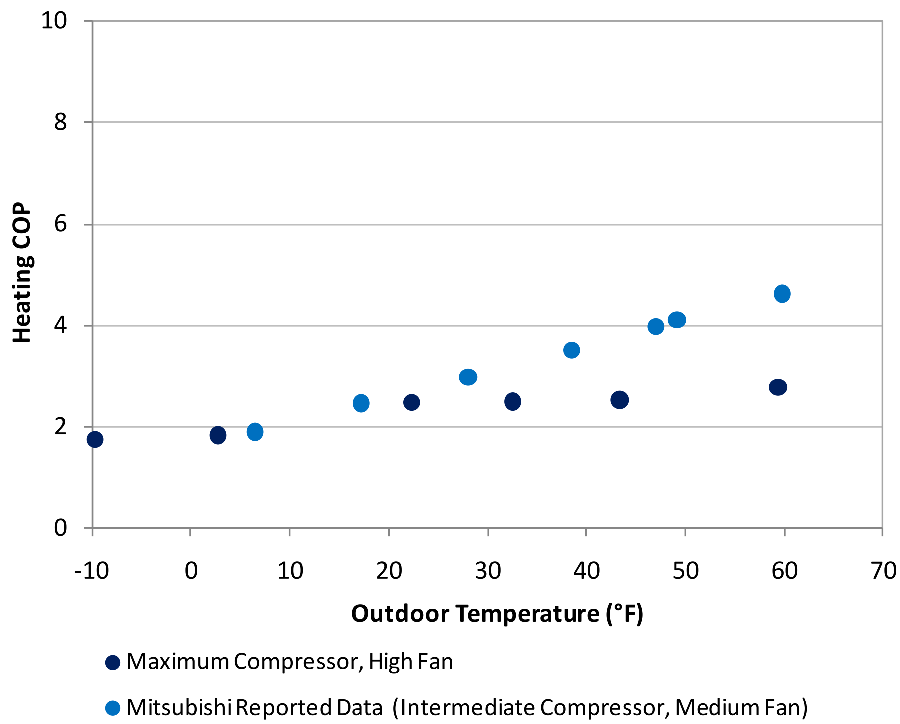

Figure 10. Mitsubishi FE12NA heating COP compared to manufacturer-reported data (70°F return temperature)

Source: Mitsubishi 2009b

4.3 Defrost Cycle

Under certain operating conditions, the heat pump must enter a defrost cycle to melt ice accumulated on the outdoor heat exchanger.

NREL/PIX 19342 (left), 19341 (right)
Credit: Howard Cheung/Herrick Labs

Figure 11. Fujitsu 12LRS outdoor coil immediately prior to defrost operation (left) and outdoor coil immediately following defrost operation (right)

Both heat pumps use a reverse cycle strategy to defrost the outdoor coil. When operating in defrost mode, the compressor pumps hot refrigerant vapor through the outdoor coil, melting ice that has accumulated on the coil. During this time, the indoor fan is disabled and the heat pump does not provide heating capacity. The defrost cycle reduces the integrated performance of the heat pump since there are periods of operation when the compressor is running but heat is not being delivered from the unit. AHRI Standard 210/240 dictates that the second defrost cycle be used to determine the defrost penalty to account for remaining moisture/frost not removed during the first defrost cycle (AHRI 2008). Each unit implements slightly different defrost control strategies as a function of outdoor temperature, run time, and refrigerant pressures.

Defrost test results for both heat pumps are shown in Table 3. Several of the Mitsubishi FE12NA steady-state tests entered defrost mode, providing defrost results for additional operating conditions. However, only a single defrost cycle was run for these particular tests. Such operating conditions had to be re-run at a lower outdoor humidity to acquire steady-state data. The differences in control strategies are evident. The Mitsubishi unit, under most operating conditions, entered the defrost cycle for a short period of time and waited a short period of time in between cycles. The defrost strategy implemented by the Mitsubishi unit also made it difficult to attain steady state data under certain operating conditions. As expected, the test conducted at a –3°F outdoor temperature required substantially more time in the defrost cycle to overcome the colder temperatures and melt the accumulated ice. Warmer outdoor temperatures (above 35°F) at higher humidity levels than the steady-state tests were tested, but the heat pumps would not enter a defrost cycle under such conditions.

Table 3. Defrost Test Results

MSHP	Test Code	Total Cycle Time (min)	Defrost Time (min)	Integrated Cycle COP	Integrated Heating COP	Defrost COP Penalty
12RLS	H-DF-35-M-MX	117	10.3	3.26	3.38	3.5%
	H-DF-17-M-MX	142	14.9	2.90	3.06	5.0%
FE12NA	H-DF-35-M-MX	90	3.3	1.76	1.78	1.4%
	H-SS-27-H-MX	79	2.0	1.72	1.74	1.3%
	H-SS-17-H-MX	91	3.8	2.24	2.28	1.8%
	H-SS-17-M-MX	90	3.3	0.88	0.89	1.4%
	H-SS-7-H-MX	31	2.2	1.08	1.13	4.7%
	H-SS-7-L-MX	23	2.5	1.53	1.60	3.9%
	H-SS-n3-H-MX*	47	10.2	1.35	1.52	11.5%

* "n" denotes negative (n3 = –3)

Cycling Tests

Unlike single-speed heat pumps, mini-split heat pumps rarely cycle between on and off. The variable speed control of MSHPs allows the unit to throttle down the capacity in lieu of turning the unit off under most operating conditions. However, as indicated by Table 1, each MSHP can only turn down the heating output to approximately 3,000 Btu/h and the unit must cycle on and off to meet heating loads below this tolerance. The cycling test results are displayed in Table 4.

Table 4. Cycling Test Results

MSHP	Test Code	Steady-State Heating Capacity (Btu/h)	Cyclic Integrated Heating Capacity (Btu)	Steady-State COP	Cyclic COP	C_d
12RLS	H-CY-62-H-MX	22,554	3,958	3.69	3.63	0.02
	H-CY-62-L-MN	6,380	1,433	7.23	5.69	0.27
FE12NA	H-CY-62-H-MX	20,234	3,583	3.01	2.70	0.12
	H-CY-62-L-MN	7,950	1,433	4.04	2.54	0.45

Both units have better cycling performance when starting up under full load conditions, however, starting up under a low load condition is more likely to occur unless the unit is recovering from a thermostat setback period. The degradation coefficients (C_d) listed in Table 4 are high compared to conventional single-speed systems. The transient startup behavior observed in the laboratory can explain the high degradation coefficients. Both units overshoot the minimum load by running the compressor at a higher speed than required for a short period of time resulting low cyclic COPs. After this initial spike, the compressor speed is turned down to low load operation. This behavior results in high degradation coefficients whenever the unit starts up under a low load. Startup data show that the FE12NA ramps the compressor higher than the 12RLS, explaining the larger C_d values.

5 Cooling Test Results

5.1 Steady State – Fujitsu 12RLS

The steady-state cooling capacities are plotted in Figure 12. All points plotted in Figure 12 were tested at standard return conditions of 80°F dry-bulb temperature and 67°F wet-bulb temperature. Test points at other return conditions are included in Table 9. As indicated in Table 1, the rated cooling capacity of this particular unit is 12,000 Btu/h (at 95°F outside temperature) with a cooling capacity that ranges from 3,800 to 14,500 Btu/h. At a high fan speed and maximum compressor load, the experimental cooling capacity was 16,400 Btu/h at 95°F (13% larger than the maximum reported capacity of 14,500 Btu/h). Similar to previous plots, a trend line has been drawn corresponding to high fan speed and maximum compressor speed operation. The rated capacity of 12,000 Btu/h can be achieved at temperatures exceeding 115°F. Though the manufacturer reports a minimum cooling capacity of 3,800 Btu/h, a cooling capacity below 5,000 Btu/h was not achieved in the laboratory. Literature provided by the manufacturer was consulted prior to testing to ensure minimum compressor speeds were achieved, however, the actual compressor speed achieved during testing could not be measured. We have developed a procedure to directly measure compressor speed in future testing.

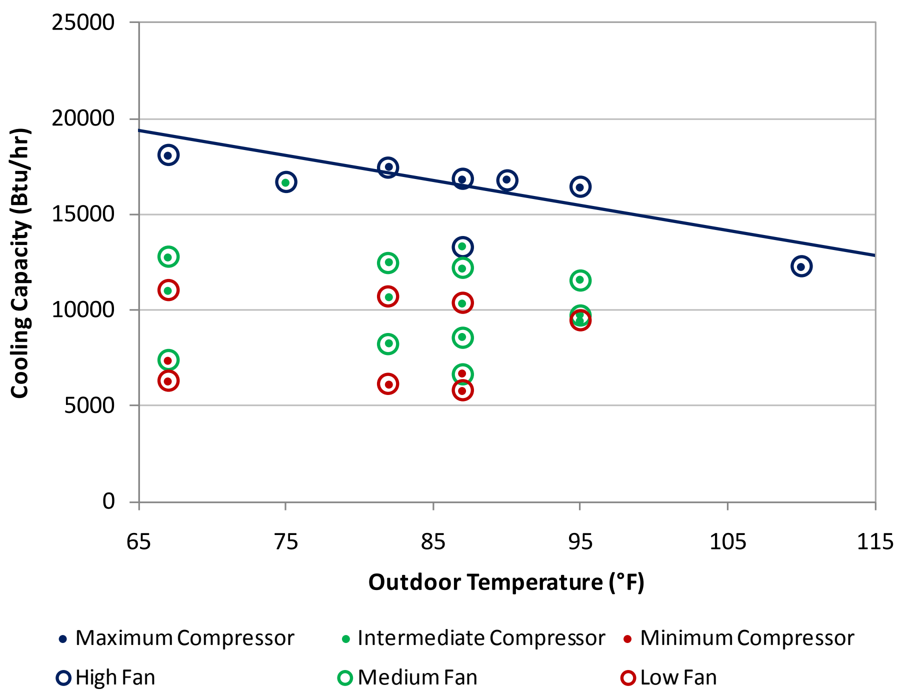

Figure 12. Fujitsu 12RLS steady-state total cooling capacity (80°F DB, 67°F WB return condition)

Figure 13 compares the manufacturer-reported data to the experimental test results. The manufacturer data are for the maximum airflow rate at an intermediate compressor load but it is compared to the maximum compressor load data from the experimental tests. As expected, the cooling capacity decreases with increasing outdoor temperature. The capacity degradation with increasing outside temperature is similar between the experimental and manufacturer-reported data.

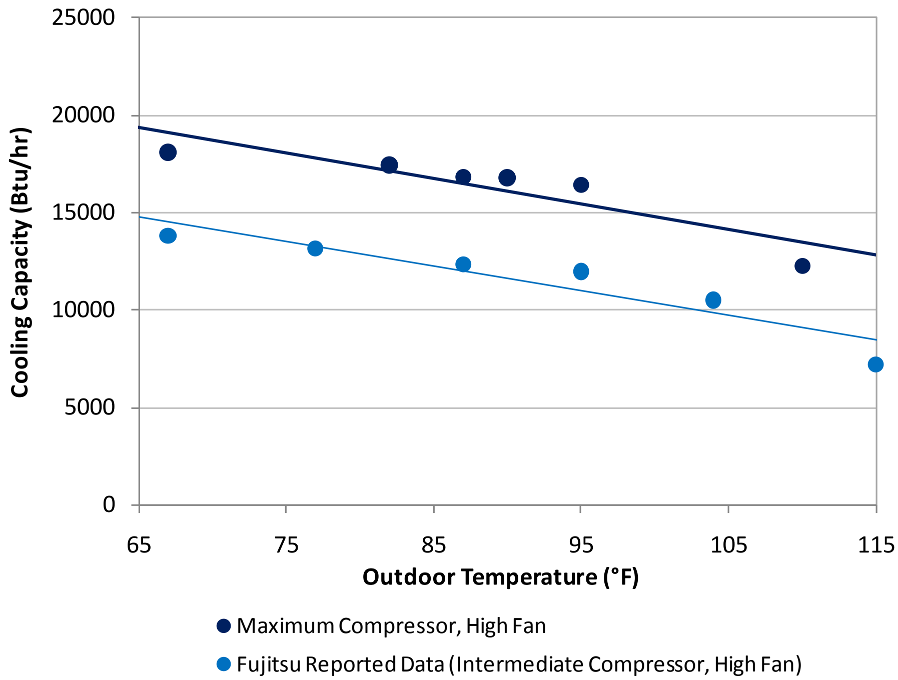

Figure 13. Fujitsu 12RLS maximum steady-state total cooling capacity compared to manufacturer-reported data (80°F DB, 67°F WB return condition)

Source: Fujitsu 2009

Figure 14 displays the COPs for the Fujitsu 12RLS steady-state cooling tests at an 80°F dry-bulb, 67°F wet-bulb return condition. COPs for other return conditions are listed in Table 9 located in Appendix A. As expected, the COP decreases at higher outdoor temperatures and larger compressor loads. The rated COP of the 12RLS is 4.24 (corresponding to an energy-efficiency ratio of 14.46, as listed in Table 1) at an outdoor temperature of 95°F which falls in the range of COPs achieved in the laboratory. The COP for maximum compressor load and high fan speed are compared to manufacturer-reported data in Figure 15. The COPs reported by the manufacturer are for a high fan speed at an intermediate compressor load and align with the results displayed in Figure 14.

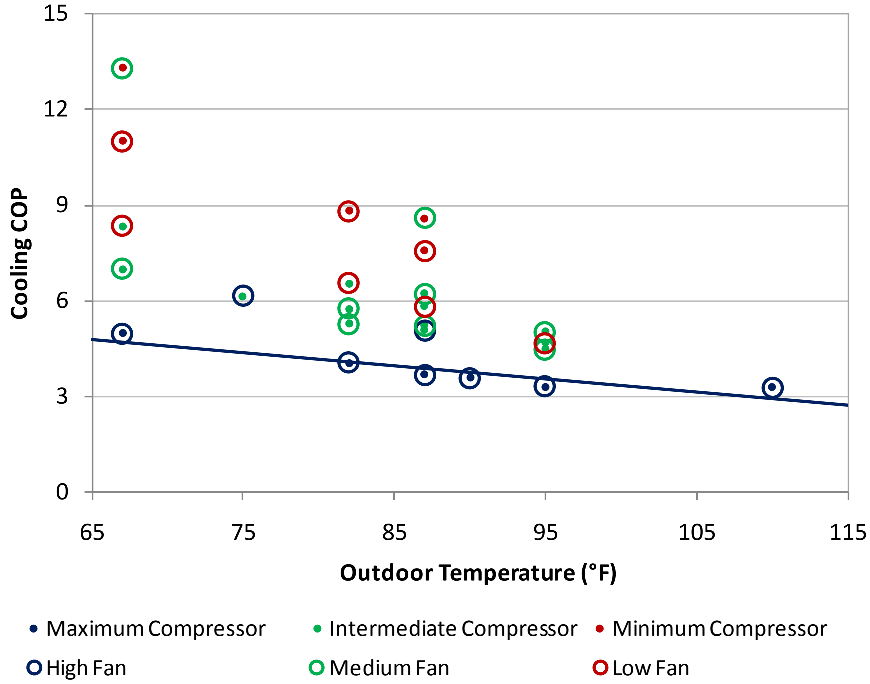

Figure 14. Fujitsu 12RLS steady-state cooling COP (80°F DB, 67°F WB return condition)

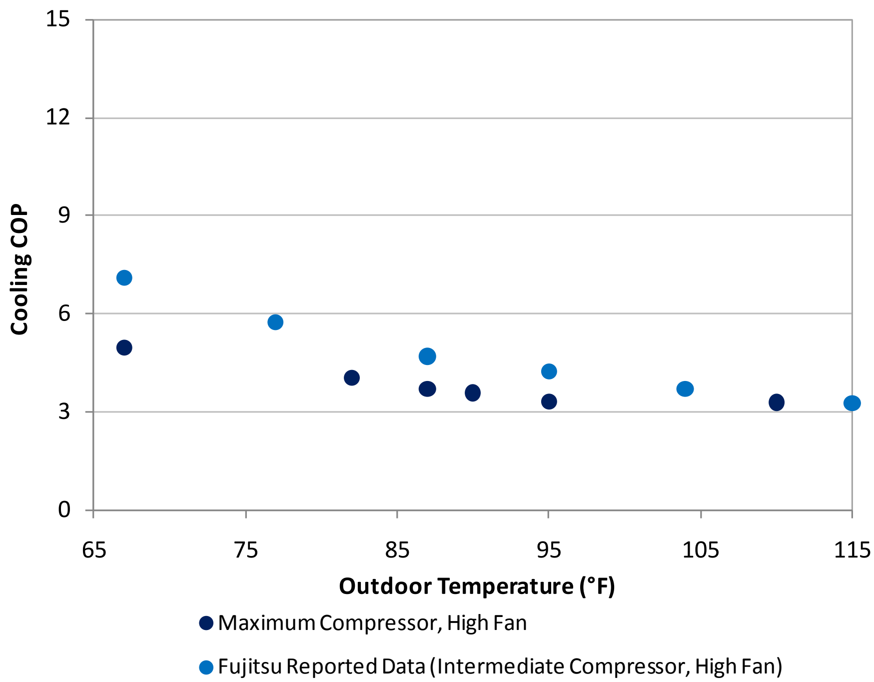

Figure 15. Fujitsu 12RLS steady-state cooling COP compared to manufacturer-reported data (80°F DB, 67°F WB return condition)

Source: Fujitsu 2009

5.2 Steady State – Mitsubishi FE12NA

Steady-state cooling capacities at the standard return conditions are plotted in Figure 16. Additional test points are listed in Appendix A. The Mitsubishi FE12NA was tested under a larger number of operating conditions than the 12RLS to refine the cooling performance model currently under development; however, the Fujitsu 12RLS was tested for more points at the standard return condition of 80°F dry-bulb, 67°F wet-bulb. The manufacturer-rated cooling capacity at a 95°F outdoor temperature is 12,000 Btu/h and the laboratory tested capacity at this condition is within the experimental uncertainty of the rated capacity. The maximum capacity listed in Table 1 for the FE12NA is 12,000 Btu/h, thus it appears that the manufacturer-reported capacities are at full compressor load conditions. Unlike the 12RLS, the FE12NA does not have the capability of providing excess cooling capacity above the rated value. This is likely the reason for a lower SEER compared to the 12RLS.

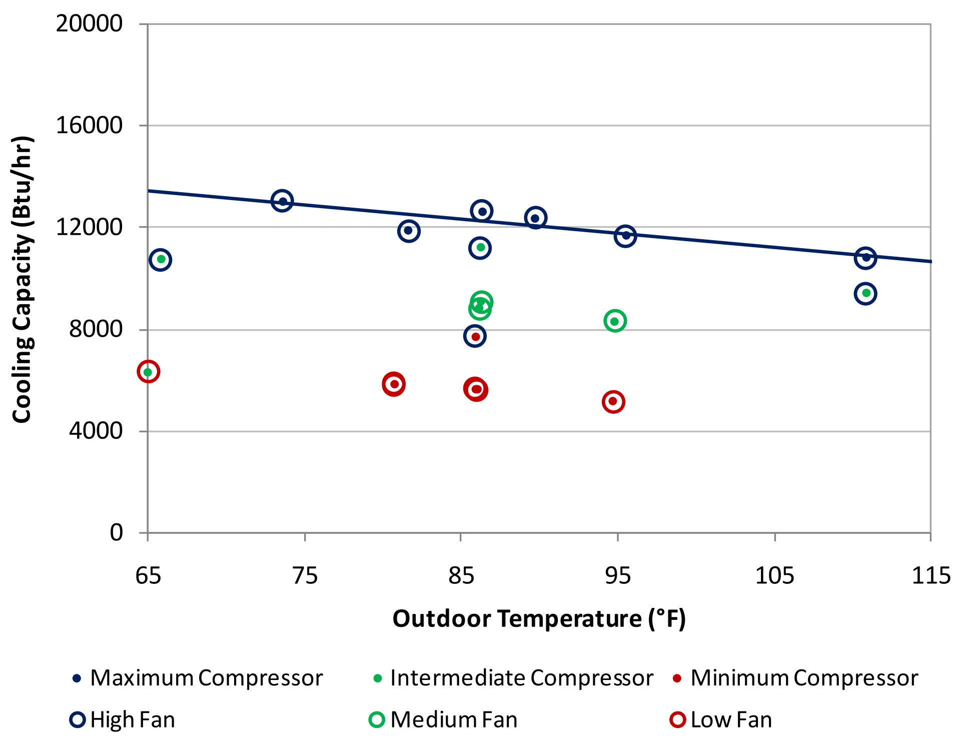

Figure 16. Mitsubishi FE12NA steady-state total cooling capacity (80°F DB, 67°F WB return condition)

Figure 17 compares the manufacturer-published performance data to the experimental test data for a variety of outdoor temperatures. The experimental results agree closely with the manufacturer-reported values.

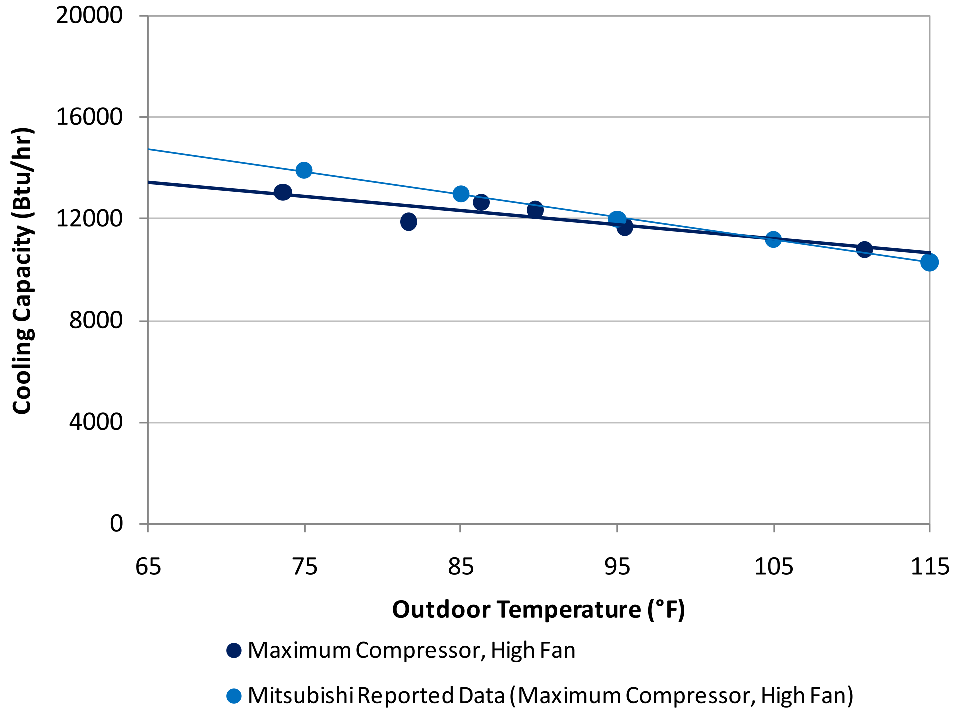

Figure 17. Mitsubishi FE12NA maximum steady-state total cooling capacity compared to manufacturer-reported data (80°F DB, 67°F WB return condition)

Source: Mitsubishi 2009b

The cooling coefficients of performance for the standard return conditions are plotted in Figure 18. The FE12NA and 12RLS have similar performance under full load conditions. The FE12NA performs slightly better than the 12RLS at higher outdoor temperatures; despite the lower seasonal energy-efficiency ratio. The higher SEER for 12RLS is due to the unit's performance at lower compressor loads. The COP for the FE12NA is not significantly dependent on the compressor load; whereas the 12RLS COP was significantly higher under low compressor loads. This can be concluded by observing the difference in scatter between Figure 14 and Figure 18.

Figure 19 compares the maximum compressor, high fan speed experimental test data to the manufacturer-reported data (Mitsubishi 2009b). The experimental and manufacturer reported data closely align.

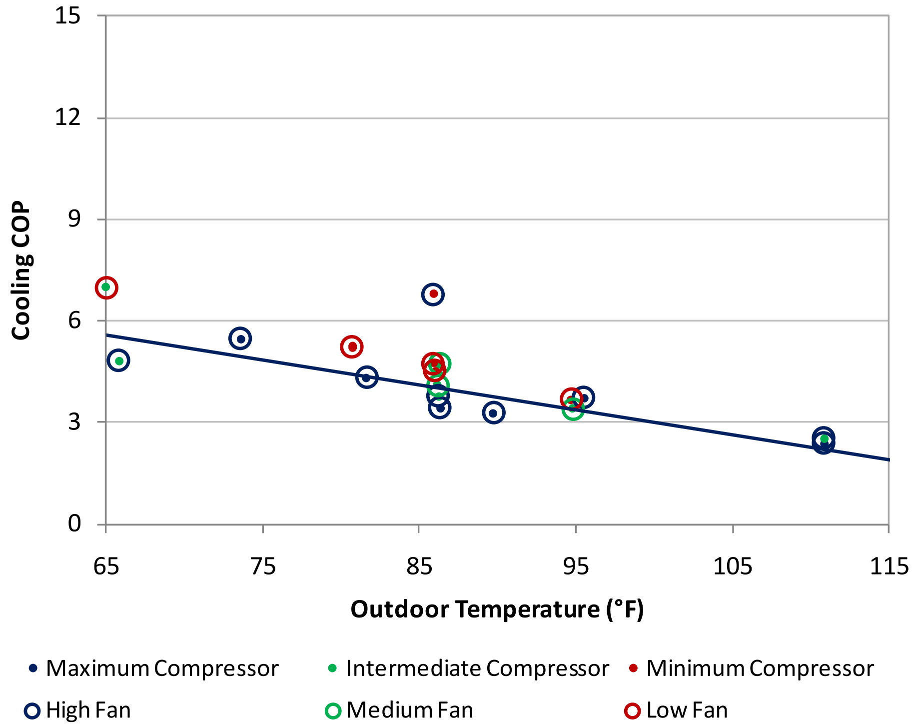

Figure 18. Mitsubishi FE12NA steady-state cooling COP (80°F DB, 67°F WB return condition)

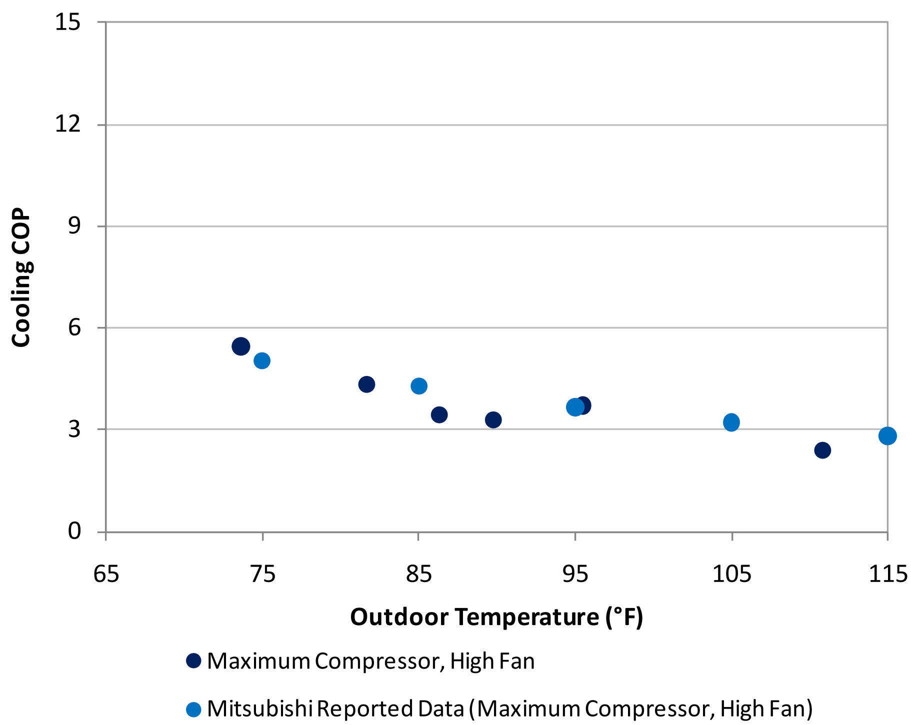

Figure 19. Mitsubishi FE12NA steady-state cooling COP compared to manufacturer-reported data (80°F DB, 67°F WB return condition)

Source: Mitsubishi 2009b

5.3 Cycling Tests

Similar to the heating cycling tests, two cycling tests were conducted for each MSHP. AHRI Standard 210/240 mandates that the unit be cycled from off to low power at an outdoor temperature of 67°F (AHRI 2008). The second test was conducted at the same outdoor temperature, however, the unit was cycled from off to maximum power. The tests concluded that both units perform better when cycling on under full load conditions. Actually, turning both units on under full load conditions resulted in negative degradation coefficients because the average coefficient of performance during the cycling test was slightly higher than the corresponding steady-state COP achieved during the steady-state test.

The degradation coefficient for the Fujitsu 12RLS turning on under low load conditions was 0.43. Despite the laboratory’s best efforts, a degradation coefficient for the Mitsubishi FE12NA could not be determined due to testing difficulties. The FE12NA cycled on to a lower load than what could be achieved during steady-state testing, resulting in a higher COP. A higher COP during cycling operation compared to steady-state operation resulted in a negative degradation coefficient.

6 Conclusions

The Fujitsu 12RLS and Mitsubishi FE12NA mini-split heat pumps have been tested over a broad range of operating conditions in the laboratory. The variable speed nature of both systems was displayed by achieving a wide range of capacities for a given outdoor temperature. The data achieved in the laboratory matched the manufacturer-reported data reasonably well.

The coefficient of performance of both systems was comparable to high SEER forced air systems. The high SEER air-conditioning systems selected for comparison were two-stage, SEER 21 systems manufactured by leading U.S. manufacturers. Low stage cooling capacities of these systems are approximately 75-80% of high stage cooling capacities. The COPs of both MSHP systems at intermediate loads were nearly equivalent (-15% – 8%) to the low stage COPs of high SEER forced air systems. However, the cooling COPs of the high SEER forced air systems were approximately 10% – 25% higher than the two MSHPs tested. Therefore at equal cooling capacities, MSHPs may not offer peak load savings compared to high SEER forced air systems. However, the potential zoning control offered by mini-split heat pumps could lead to an overall peak load reduction.

Two-stage forced air systems must cycle on and off at loads below the low stage cooling capacity. MSHPs can reduce the compressor speed to meet low cooling loads and have higher COPs under such conditions. Whole-building simulations are required to compare annual energy usage between MSHPs and forced air systems. The test data collected in the laboratory will facilitate the development of a MSHP component model for use in whole-building simulation tools and ultimately be used to compare the annual energy use of MSHPs to high performing single and two stage systems.

References

AHRI. (2008). Performance Rating of Unitary Air-Conditioning and Air-Source Heat Pump Equipment. AHRI Standard 210/240-2008. Arlington, VA: Air-Conditioning, Heating, and Refrigeration Institute.

ASHRAE. (1987). Standard Methods for Laboratory Airflow Measurement. ASHRAE Standard 41.2-1987. Atlanta, GA: American Society of Heating, Refrigerating, and Air-Conditioning Engineers.

ASHRAE. (2010). Methods of Testing for Rating Seasonal Efficiency of Unitary Air-Conditioners and Heat Pumps. ASHRAE Standard 116-2010. Atlanta, GA: American Society of Heating, Refrigerating, and Air-Conditioning Engineers.

Christensen, D.; Fang, F.; Tomerlin, J.; Winkler, J.; Hancock, E. (2011). Field Monitoring Protocol: Mini-Split Heat Pumps. National Renewable Energy Laboratory: Golden, CO.

Fujitsu. (2009). Design and Technical Data for Models: Indoor Unit ASU9RLS & ASU12RLS, Outdoor Unit AOU9RLS & AOU12RLS. No D2D_AS037E/01. Japan: Fujitsu General Limited.

Larson, B.; Baylon, D.; Storm, P. (2011). Ductless Heat Pump Impact & Process Evaluation: Lab-Testing Report. Ecotope, Inc.: Seattle, WA.

Mitsubishi Electric Corporation. (2009a). Indoor Unit Service Manual for Models MSZ-FE09NA & MSZ-FE12NA. No OBH542. Japan: Mitsubishi Electric Corporation.

Mitsubishi Electric Corporation. (2009b). Outdoor Unit Service Manual for Models MUZ-FE09NA & MUZ-FE12NA. No OBH543. Japan: Mitsubishi Electric Corporation.

Appendix A–Mini-Split Heat Pump Laboratory Test Results

Table 5. Fujitsu 12RLS Steady-State Heating Test Results

Test Code	Indoor Temperature (°F)	Heating Capacity (Btu/h)	Indoor Unit Fan Power (W)	Outdoor Unit Total Power (W)	COP	Indoor Coil Airflow Rate (cfm)	Supply Air Temperature (°F)
H-SS-65-H-MN	69.7	7,145	12.0	208	9.53	414	86.3
H-SS-62-H-MX	68.9	22,571	34.0	1,760	3.69	418	123.3
H-SS-62-M-MX	69.2	19,986	23.2	1,523	3.79	347	127.2
H-SS-62-M-INT	69.0	14,060	22.9	816	4.91	347	109.2
H-SS-62-M-MN	69.4	6,789	10.3	226	8.42	347	88.3
H-SS-62-L-MX	69.5	15,778	13.5	1,238	3.69	252	132.4
H-SS-62-L-INT	69.2	10,481	13.5	604	4.98	251	110.4
H-SS-62-L-MN	69.5	6,380	8.5	250	7.22	252	94.1
H-SS-47-H-MX	68.4	20,600	34.6	1,893	3.13	413	119.5
H-DF-47-M-MX	68.6	16,673	23.7	1,310	3.66	348	115.8
H-SS-47-L-MX	68.9	12,872	14.1	1,080	3.45	249	121.4
H-SS-47-L-INT	69.3	4,402	8.2	238	5.24	248	86.7
H-SS-35-H-MX	68.8	19,060	31.7	2,126	2.59	421	117.2
H-SS-35-M-INT	68.9	13,852	23.7	1,178	3.38	349	108.0
H-SS-35-L-MN	69.3	6,448	9.7	405	4.56	247	94.5
H-SS-27-H-MX	69.0	19,132	34.0	2,163	2.53	450	112.6
H-SS-27-H-INT	69.2	17,038	33.4	1,791	2.72	441	108.6
H-SS-27-M-INT	69.3	12,879	17.0	1,152	3.16	343	107.3
H-SS-27-L-MX	69.6	9,921	14.4	916	3.12	252	108.7
H-SS-17-H-MX	68.8	16,939	32.5	2,159	2.27	416	110.7
H-SS-17-H-INT	68.9	13,732	32.5	1,512	2.63	416	102.6
H-SS-17-M-INT	69.1	10,990	17.3	1,049	2.99	355	100.4

Table 5. Fujitsu 12RLS Steady-State Heating Test Results (continued)

Test Code	Indoor Temperature (°F)	Heating Capacity (Btu/h)	Indoor Unit Fan Power (W)	Outdoor Unit Total Power (W)	COP	Indoor Coil Airflow Rate (cfm)	Supply Air Temperature (°F)
H-SS-15-M-MX	69.2	10,519	24.0	1,025	2.94	348	98.8
H-SS-7-H-MX	69.4	17,110	22.0	2,166	2.27	452	107.4
H-SS-7-L-MX	69.9	7,343	10.3	774	2.74	253	98.0
H-SS-n3-H-MX	70.1	12,214	14.6	1,915	1.87	416	97.3
H-SS-62-H-MX-60	58.5	23,418	31.4	1,766	3.82	417	113.6
H-SS-62-H-MX-75	74.1	21,408	34.6	1,795	3.43	420	125.1
H-SS-47-L-MX-75	74.1	12,710	13.3	1,152	3.20	256	123.3
H-SS-35-M-MX-65	63.4	13,939	23.7	1,173	3.41	349	102.2
H-SS-27-H-MX-75	73.8	17,276	34.8	2,134	2.32	418	115.0
H-SS-27-H-MX-60	57.8	17,443	35.6	2,115	2.39	417	98.7

Table 6. Mitsubishi FE12NA Steady-State Heating Test Results

Test Code	Outdoor Temperature (°F)	Indoor Temperature (°F)	Heating Capacity (Btu/h)	Indoor Unit Fan Power (W)	Outdoor Unit Total Power (W)	COP	Indoor Coil Airflow Rate (cfm)	Supply Air Temperature (°F)
H-SS-62-H-MX	59.4	69.1	19,995	23.5	2,082	2.78	335	130.0
H-SS-62-H-MN	59.4	69.6	9,963	22.5	528	5.31	316	100.2
H-SS-62-M-MX	59.4	70.6	11,533	9.5	991	3.38	211	124.8
H-SS-62-M-INT	59.5	70.0	7,268	9.4	406.5	5.11	211	103.5
H-SS-62-L-MX	59.6	69.4	8,906	5.9	871.8	2.97	142	131.4
H-SS-62-L-MN	59.6	67.5	7,950	5.6	570	4.04	150	119.7
H-SS-47-H-MX	43.4	67.8	19,040	23.7	2,184	2.53	336	123.7
H-SS-47-M-MN	43.6	66.6	14,911	17.2	1,662	2.6	256	123.7
H-SS-47-L-INT	43.8	67.2	9,042	5.7	882	2.99	150	126.6
H-SS-47-L-MN	44.0	66.5	9,759	5.8	1,161	2.45	145	132.6
H-SS-35-H-MX	32.6	68.0	18,289	24.1	2,118	2.5	335	121.9
H-SS-35-M-MX	30.8	68.8	13,614	9.4	1,688	2.35	217	131.4
H-SS-35-M-INT	31.0	68.5	16,105	19.4	2,003	2.33	299	121.3
H-SS-35-L-MX	30.6	68.8	9,656	6.0	1,335	2.11	155	130.4
H-SS-35-L-MN	30.2	69.3	9,281	6.0	1,300	2.09	152	129.9
H-SS-27-H-MX	22.3	68.5	16,310	22.9	1,900	2.48	340	116.1
H-SS-27-L-MX	22.9	68.7	9,520	5.8	1,590	1.75	154	130.0
H-SS-27-L-MN	23.0	68.7	9,929	5.8	1,444	2.01	154	132.6
H-SS-17-M-INT	14.9	69.9	10,475	9.4	1,445	2.11	210	119.3
H-SS-7-H-MX	2.8	68.0	9,793	21.6	1,540	1.84	340	95.3
H-SS-7-L-MX	2.8	67.4	8,530	6.1	1,874	1.33	159	119.7
H-SS-n3-H-MX*	-9.7	67.5	7,165	25.0	1,174	1.75	334	88.1

* “n” denotes negative (n3 = –3)

Table 6. Mitsubishi FE12NA Steady-State Heating Test Results (continued)

Test Code	Outdoor Temperature (°F)	Indoor Temperature (°F)	Heating Capacity (Btu/h)	Indoor Unit Fan Power (W)	Outdoor Unit Total Power (W)	COP	Indoor Coil Airflow Rate (cfm)	Supply Air Temperature (°F)
H-SS-62-H-MX-75	60.8	74.4	19,074	23.7	1,877	2.94	343	130.2
H-SS-62-H-INT-75	61.5	73.6	16,105	23.7	1,388	3.34	336	121.2
H-SS-62-H-MX-60	60.4	58.3	24,294	23.9	2,321	3.04	343	129.4
H-SS-62-L-MX-60	59.5	67.4	7,370	5.7	987.1	2.18	131	122.0
H-SS-47-H-MX-75	43.6	74.2	19,313	23.3	2,191	2.56	340	130.6
H-SS-47-H-MN-75	44.2	74.0	3,651	26.8	193	4.86	341	84.3
H-SS-47-L-INT-75	43.8	73.2	7,063	5.7	625	3.28	151	119.3
H-SS-35-M-MX-64	30.9	61.4	15,798	9.6	2,088	2.21	217	134.1
H-SS-35-M-INT-64	30.8	62.7	14,911	9.7	1,570	2.77	240	123.9
H-SS-35-H-MX-60	30.8	58.3	18,630	23.6	1,880	2.87	340	110.5
H-SS-35-H-MX-60	30.8	56.9	18,357	24.6	1,847	2.88	342	109.2
H-SS-27-H-MX-60	22.2	59.3	15,628	25.3	1,682	2.68	342	103.6

Table 7. Fujitsu 12RLS Steady-State Cooling Test Results

Test Code	Indoor Dry-Bulb Temperature (°F)	Indoor Wet-Bulb Temperature (°F)	Total Cooling Capacity (Btu/h)	Sensible Heat Ratio	Indoor Unit Fan Power (W)	Outdoor Unit Total Power (W)	COP	Indoor Coil Airflow Rate (cfm)	Supply Air Temperature (°F)
C-SS-110-H-MX	79.8	65.5	12,291	0.89	39.0	1,057	3.29	475	57.5
C-SS-095-H-MX	80.0	65.7	16,424	0.77	38.4	1,408	3.33	475	53.9
C-SS-095-M-INT	79.8	65.2	11,571	0.85	25.5	730	4.49	389	55.1
C-SS-095-M-INT	79.9	65.6	9,744	0.92	25.5	542	5.04	389	57.5
C-SS-095-L-INT	79.2	65.1	9,467	0.8	14.9	579	4.68	290	53.7
C-SS-090-H-MX	79.2	65.2	16,789	0.76	38.4	1,334	3.58	475	52.9
C-SS-087-H-MX	79.3	65.3	16,837	0.75	38.4	1,296	3.7	475	53.0
C-SS-087-H-INT	79.3	65.3	13,295	0.84	38.4	727	5.09	476	56.2
C-SS-087-M-INT	79.4	65.4	12,196	0.8	25.2	656	5.24	391	54.8
C-SS-087-M-INT	79.4	65.3	8,593	0.96	24.6	380	6.23	391	58.5
C-SS-087-L-MN	80.7	66.9	5,792	0.98	14.1	210	7.57	284	61.3
C-SS-087-L-INT	79.4	65.1	10,379	0.75	13.8	508	5.83	287	53.0
C-SS-087-M-MN	79.6	65.3	6,684	0.9	24.3	204	8.59	386	64.5
C-SS-082-H-MX	78.7	64.9	17,448	0.74	38.7	1,220	4.06	472	52.1
C-SS-082-M-INT	78.7	64.8	12,496	0.8	25.5	610	5.76	391	53.9
C-SS-082-M-INT	78.7	63.9	8,231	0.87	24.6	432	5.29	391	55.9
C-SS-082-L-MN	79.1	65.4	6,140	0.92	14.1	190	8.83	283	59.6
C-SS-082-L-INT	80.8	66.8	10,707	0.73	13.8	465	6.56	282	53.8
C-SS-075-H-INT	80.9	67.0	16,690	0.73	38.4	756	6.16	475	55.7
C-SS-067-H-MX	79.2	65.1	18,107	0.73	38.1	1,026	4.98	473	51.6
C-SS-067-M-INT	79.2	65.2	12,756	0.78	24.3	510	7	388	53.9
C-SS-067-M-MN	79.1	65.1	7,370	1	24.3	138	13.3	390	60.2
C-SS-067-L-INT	79.7	65.8	11,014	0.71	13.8	373	8.35	287	53.2

Table 7. Fujitsu 12RLS Steady-State Cooling Test Results (continued)

Test Code	Indoor Dry-Bulb Temperature (°F)	Indoor Wet-Bulb Temperature (°F)	Total Cooling Capacity (Btu/h)	Sensible Heat Ratio	Indoor Unit Fan Power (W)	Outdoor Unit Total Power (W)	COP	Indoor Coil Airflow Rate (cfm)	Supply Air Temperature (°F)
C-SS-067-L-MN	79.8	66.0	6,298	0.92	14.1	154	11	287	60.0
C-SS-052-H-INT	81.0	66.2	13,452	0.86	37.2	323	10.93	475	57.2
C-SS-057-H-INT	81.3	66.6	13,295	0.86	37.2	375	9.45	475	57.8
C-SS-062-H-INT	81.3	66.9	13,480	0.83	37.2	416	8.71	475	58.1
C-SS-067-H-MX-D	80.0	54.3	17,458	1	40.4	1,013	4.86	476	46.3
C-SS-067-L-MN-D	79.5	54.2	6,653	1	14.4	125	13.96	288	61.2
C-SS-67-H-MX-60	78.3	60.2	16,924	0.95	41.1	1,037	4.51	564	47.3
C-SS-80-M-MX-60	78.3	60.9	11,635	0.99	26.1	604	5.7	424	50.7
C-SS-67-H-MX-70	78.4	68.8	18,323	0.62	39.7	1,052	5.07	553	56.5
C-SS-95-H-MX-70	80.1	70.4	16,685	0.64	41.0	1,425	3.35	487	59.7
C-SS-95-H-MX-60	79.5	61.7	15,355	0.98	42.0	1,406	3.01	487	51.4

Table 8. Mitsubishi FE12NA Steady-State Cooling Test Results

Test Code	Outdoor Temp. (°F)	Indoor Dry-Bulb Temp. (°F)	Indoor Wet-Bulb Temp. (°F)	Total Cooling Capacity (Btu/h)	Sensible Heat Ratio	Indoor Unit Fan Power (W)	Outdoor Unit Total Power (W)	COP	Indoor Coil Air Flow Rate (cfm)	Supply Air Temp. (°F)
C-SS-110-H-MX	110.8	80.4	65.4	10,816	0.83	24	1,330	2.38	340	55.9
C-SS-110-H-INT	110.8	80.4	65.4	9,407	0.89	23	1,081	2.54	341	57.7
C-SS-095-H-MX	95.5	79.7	64.7	11,687	0.81	22	905	3.72	337	53.4
C-SS-095-M-INT	94.8	79.9	64.7	8,336	0.76	8	656	3.40	190	51.1
C-SS-095-L-MN	94.7	80.6	64.9	5,156	0.77	5	449	3.68	141	51.8
C-SS-090-H-MX	89.7	79.5	64.4	12,369	0.78	23	1,071	3.28	332	53.1
C-SS-087-H-MX	86.3	79.3	64.1	12,642	0.78	22	1,032	3.43	326	52.2
C-SS-087-L-MN	85.9	80.2	65.3	5,654	0.72	5	395	4.74	145	50.5
C-SS-087-H-INT	86.3	79.3	64.1	11,199	0.83	23	828	3.77	327	53.8
C-SS-087-M-INT	86.2	79.0	63.9	8,817	0.76	8	574	4.10	189	49.1
C-SS-087-M-INT	86.3	80.6	65.0	9,097	0.74	8	567	4.73	209	50.4
C-SS-087-H-MN	85.9	80.4	65.4	7,718	0.96	22	316	6.78	340	59.9
C-SS-087-L-MN	86.0	80.6	65.0	5,623	0.73	5	397	4.53	141	50.5
C-SS-082-H-MX	81.7	79.7	64.7	11,884	0.79	22	787	4.33	337	53.6
C-SS-082-M-INT	81.6	81.0	65.9	9,854	0.71	8	540	5.34	208	49.6
C-SS-082-L-MN	80.7	80.6	65.0	5,879	0.73	5	368	5.24	144	49.5
C-SS-082-L-MN	80.7	80.6	65.1	5,852	0.72	5	368	5.21	144	49.8
C-SS-075-H-MX	73.6	80.4	65.1	13,051	0.76	23	689	5.46	340	53.1
C-SS-067-H-INT	65.8	79.7	64.8	10,762	0.79	22	639	4.81	337	56.1
C-SS-067-L-INT	65.0	80.6	65.0	6,336	0.70	5	296	6.98	144	48.2
C-SS-095-H-MX-65	94.5	80.2	63.1	11,983	0.87	23	879	3.98	342	51.4
C-SS-089-H-MX-65	87.9	80.4	63.2	12,318	0.85	22	814	4.39	341	51.6
C-SS-087-H-MX-65	85.7	80.1	62.9	12,011	0.86	23	795	4.40	342	51.6

Table 8. Mitsubishi FE12NA Steady-State Cooling Test Results (continued)

Test Code	Outdoor Temp. (°F)	Indoor Dry-Bulb Temp. (°F)	Indoor Wet-Bulb Temp. (°F)	Total Cooling Capacity (Btu/h)	Sensible Heat Ratio	Indoor Unit Fan Power (W)	Outdoor Unit Total Power (W)	COP	Indoor Coil Air Flow Rate (cfm)	Supply Air Temp. (°F)
C-SS-083-H-MX-65	81.6	80.2	63.2	11,052	0.85	23	755	4.25	342	54.1
C-SS-075-L-INT-58	73.5	81.0	61.5	6,200	0.83	5	338	5.53	133	43.5
C-SS-095-H-MX-76	94.8	78.8	70.4	12,543	0.53	21	955	3.54	314	60.3
C-SS-095-H-MX-75	95.3	83.5	73.8	13,806	0.52	22	903	4.40	337	63.5
C-SS-087-H-MX-75	86.5	82.0	73.9	12,792	0.49	22	813	4.53	337	64.6
C-SS-075-H-MX-75	74.3	80.6	72.0	10,015	0.53	22	686	4.18	338	65.8
C-SS-095-H-MX-74	94.0	80.4	72.4	13,717	0.50	22	890	4.50	342	61.3
C-SS-085-H-MX-74	83.5	81.0	72.6	12,628	0.51	22	785	4.69	342	63.0
C-SS-095-H-MX-65	94.9	74.1	58.4	10,929	0.91	23	880	3.57	337	46.9
C-SS-095-H-MX-86-D	94.8	84.9	55.6	11,107	0.99	24	891	3.60	339	54.0
C-SS-087-H-MX-85-D	86.4	85.6	56.9	12,192	0.98	23	807	4.34	337	52.2
C-SS-067-H-MX-85-D	65.2	86.9	55.6	10,137	0.98	23	611	4.75	339	59.0
C-SS-095-H-MX-83-D	94.8	81.9	54.2	10,813	0.99	24	888	3.52	339	51.6
C-SS-110-H-MX-D	110.9	80.6	53.6	8,899	1.00	23	1,027	2.51	338	56.3
C-SS-095-H-MX-80-D	94.8	78.8	52.9	10,380	0.99	24	884	3.39	339	49.8
C-SS-095-L-MX-D	94.5	81.9	57.4	4,743	0.99	6	446	3.54	146	47.5
C-SS-095-H-INT-D	94.4	81.0	56.7	7,138	0.97	23	362	5.56	342	61.5
C-SS-095-M-MN-D	94.9	79.9	51.3	2,709	0.97	9	140	5.41	208	67.8
C-SS-095-L-MN-D	94.9	79.9	51.3	2,030	0.98	6	144	4.70	151	65.3
C-SS-087-M-MN-D	86.4	79.7	51.1	3,050	0.98	9	112	7.51	208	66.2
C-SS-087-L-MN-D	86.4	79.9	51.2	2,290	0.98	6	116	6.52	151	63.3
C-SS-082-H-MX-D	81.1	81.3	53.3	10,673	1.00	23	747	4.10	338	52.0
C-SS-075-H-MX-70-D	73.7	68.0	46.9	9564	1.00	23	675	4.06	338	42.1

Table 8. Mitsubishi FE12NA Steady-State Cooling Test Results (continued)

Test Code	Outdoor Temp. (°F)	Indoor Dry-Bulb Temp. (°F)	Indoor Wet-Bulb Temp. (°F)	Total Cooling Capacity (Btu/h)	Sensible Heat Ratio	Indoor Unit Fan Power (W)	Outdoor Unit Total Power (W)	COP	Indoor Coil Air Flow Rate (cfm)	Supply Air Temp. (°F)
C-SS-067-H-MX-D	65.4	80.2	56.4	9919	0.99	24	615	4.67	343	53.1
C-SS-067-L-MN-D	65.0	82.6	57.0	5,664	0.99	6	265	6.98	145	42.1
C-SS-095-H-MX-77-D	94.9	75.6	51.4	10,032	0.98	24	864	3.36	339	47.8
C-SS-073-H-MX-77-D	71.0	75.9	51.6	10,892	0.99	24	670	4.66	339	45.1
C-SS-095-H-MX-75-D	95.1	74.8	52.8	10,632	0.98	24	880	3.47	337	46.2
C-SS-087-M-MX-75-D	86.6	74.1	55.2	7,479	1.00	9	559	3.97	210	41.0
C-SS-073-H-MX-75-D	71.0	73.9	50.4	10,656	0.99	24	674	4.53	339	43.9
C-SS-095-H-MX-74-D	94.9	72.5	49.9	9,564	0.99	24	857	3.22	339	45.9
C-SS-087-H-MX-74-D	86.4	72.9	50.4	9,960	0.99	25	792	3.62	339	45.3
C-SS-073-H-MX-73-D	71.0	71.6	49.8	10,352	1.00	24	678	4.38	339	42.3
C-SS-095-H-MX-70-D	94.9	68.5	48.2	9,029	0.99	24	850	3.07	339	43.3
C-SS-082-H-INT-D	81.3	68.4	49.8	9,759	1.00	24	754	3.75	342	41.5
C-SS-082-H-MX-D	81.3	68.4	49.8	10,028	1.00	24	805	3.61	341	40.8
C-SS-075-H-MX-D	73.8	69.1	50.2	10,335	1.00	24	686	4.36	342	40.6
C-SS-082-M-INT-62	80.9	61.0	50.0	4,395	0.98	9	266	4.79	209	41.9

EERE Information Center
1-877-EERE-INFO (1-877-337-3463)
www.eere.energy.gov/informationcenter

U.S. DEPARTMENT OF ENERGY | Energy Efficiency & Renewable Energy

DOE/GO-102011-3380 ▪ September 2011